



**Michigan
Technological
University**

Michigan Technological University
Digital Commons @ Michigan Tech

Michigan Tech Publications

4-26-2022

Synthesis and Characterization of Alkyne-Functionalized Photo-Cross-Linkable Polyesters

Warrick Ma

Cornell University College of Arts and Sciences

Xiaochu Ding

Michigan Technological University, xding@mtu.edu

Ying Chen

Cornell University College of Engineering

Yadong Wang

Cornell University College of Engineering

Follow this and additional works at: <https://digitalcommons.mtu.edu/michigantech-p>

 Part of the [Chemistry Commons](#)

Recommended Citation

Ma, W., Ding, X., Chen, Y., & Wang, Y. (2022). Synthesis and Characterization of Alkyne-Functionalized Photo-Cross-Linkable Polyesters. *ACS Omega*, 7(18), 15540-15546. <http://doi.org/10.1021/acsomega.2c00272>

Retrieved from: <https://digitalcommons.mtu.edu/michigantech-p/16038>

Follow this and additional works at: <https://digitalcommons.mtu.edu/michigantech-p>

 Part of the [Chemistry Commons](#)

Synthesis and Characterization of Alkyne-Functionalized Photo-Cross-Linkable Polyesters

Warrick Ma, Xiaochu Ding,* Ying Chen, and Yadong Wang*



Cite This: *ACS Omega* 2022, 7, 15540–15546



Read Online

ACCESS |



Metrics & More

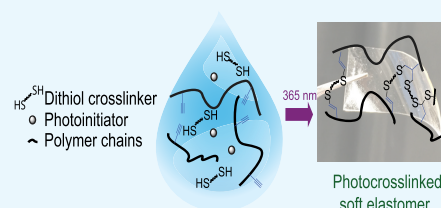


Article Recommendations



Supporting Information

ABSTRACT: An alkyne-functionalized elastomer derived from sebacic acid, 1,3-propanediol, and alkyne-functionalized serinol is synthesized via melt condensation. A low-power UV lamp triggers the cross-linking rapidly via thiol–yne click chemistry. The cross-linking behavior is studied by photorheology and NMR spectroscopy. The resultant elastomer possesses mechanical properties similar to those of human soft tissues and exhibits *in vitro* degradability and good cytocompatibility.



INTRODUCTION

Currently, light-based 3D printing for biomedical applications commonly uses methacrylic- and acrylic-based (here grouped together and termed MAA) resins because of their high reactivity and availability. This photo-cross-linking chemistry has enabled novel additive manufacturing such as digital light processing (DLP).^{1–3} However, MAA often cannot reach complete conversion because of the partially cross-linked network's limited diffusion coefficient and sensitivity of radicals to atmospheric oxygen. *In vivo*, unreacted MAA in cross-linked MAA-based resins can hydrolyze and yield free methacrylic and acrylic acids, which are sensitizing, irritating, toxic, and potentially carcinogenic.^{4,5} To develop a more biocompatible photo-cross-linkable resin, we designed a polyester that utilizes thiol–yne cross-linking chemistry with a higher oxygen tolerance.

Previously, photopolymerizable resins derived from an alkyne-generated, highly cross-linked network via DLP.^{5,6} Compared with free radical cross-linking of MAA-based resins, thiol–yne cross-linking is more tolerant to oxygen, and unconjugated alkynes are less susceptible to nucleophilic addition. In the literature, alkyne-functionalized UV cross-linkable resins mostly comprise small-molecule bifunctional alkyne monomers, which are used with multifunctional thiols to generate a highly cross-linked network.^{6,7} Because the cross-linking density correlates to the degree of conversion, and a high conversion is required to minimize the amount of leachable oligomers/monomers, such materials typically possess a high Young's modulus, rendering them unsuitable for soft material applications. In comparison, alkyne-functionalized polymer can be cross-linked by dithiols at a lower density and yield a softer material. Adopted from a previous published work by our group, we synthesized a polyester functionalized with terminal alkyne groups via melt polycondensation of sebacic acid, 1,3-propanediol, and alkyne-

functionalized serinol.⁸ We then cross-linked it with a low power UV lamp (5 mW) using thiol–yne chemistry. The material possesses mechanical properties comparable to those of human soft tissues. The polymer extract shows good cytocompatibility *in vitro* and partial degradation in basic solution in *in vitro*.

MATERIALS AND METHODS

General Experimental. All reagents were acquired commercially and used as received. Flash chromatography was performed on a Biotage Isolera using a Biotage SNAP Ultra silica gel column. TLC was performed on silica gel 60 F254 plates. NMR spectra were recorded on a Bruker 500 MHz instrument.

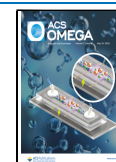
Synthesis of Alkyne-Functionalized Serinol Monomer (AK). Equimolar amount of serinol (1 mmol) and methyl 5-hexynoate (1 mmol) were added into a round-bottom flask. The mixture was stirred under nitrogen for 25 h. The crude oil was recrystallized from ethyl acetate and then purified via flash chromatography (ethyl acetate/methanol) to yield a fluffy white solid (50% yield).

Synthesis of Poly[(alkyne-serinol)-ran-(propanediol-co-sebacate)] (PAPS). Sebacic acid (100 mol %) and 1,3-propanediol (100 – *x* mol %) were added into a three-neck round-bottom flask, which was then outfitted with a gas adapter and a condenser equipped with a receiving flask. The mixture formed a melt at 135 °C was stirred at 135 °C under nitrogen gas for 24 h and then under vacuum for 24 h. To the

Received: January 13, 2022

Accepted: March 17, 2022

Published: April 26, 2022



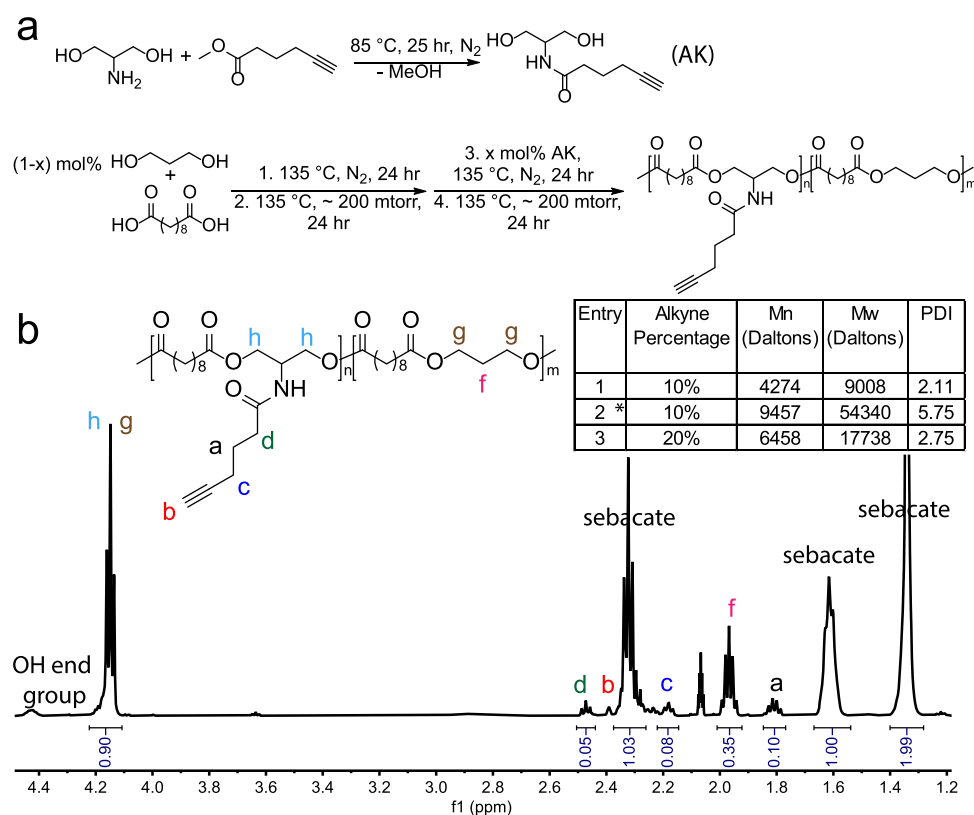


Figure 1. Synthesis and characterization of PAPS. (a) Synthesis of *N*-(5-hexynoamido)-1,3-propanediol and poly(alkyne serinol)-*ran*-propanediol-co-sebacate (PAPS). (b) ^1H NMR in acetone- d_6 and GPC characterization of 20% PAPS; residual solvent signal is at 2.05 ppm. * Extending the vacuum polycondensation step to 48 h increased the molecular weight and PDI.

reaction was then added x mol % alkyne-serinol monomer along with 30 mL of acetone, and the reaction was refluxed so all the sublimed low-molecular-weight species were rinsed back into the reaction mixture. Acetone was distilled off, and the melt was then stirred at 135 °C under nitrogen for 24 h and eventually under vacuum for 24 h. Upon cooling, the mixture solidified and was used without purification.

Resin Preparation and Photo-Cross-Linking. Dissolved in 1 mL of 1:1 EtOH/EtOAc with gentle heating were 600 mg of PAPS and 12 mg of diphenyl(2,4,6-trimethylbenzoyl)-phosphine oxide (TPO). A calculated amount of 2,2'-(ethylenedioxy)diethanethiol (dithiol) was then added via a pipet. The solution was then spread onto a mold of desired shape and cured under 5 mW 365 nm UV from 3 cm away for 10 min. The resulting slab was washed briefly with ethanol, and solvents were evaporated first in air, then under vacuum, for a few days.

Material Characterization. Gel permeation chromatography (GPC) was conducted using Malvern Panalytical OMNISEC GPC system (Malvern Instruments Ltd., Malvern, UK) via a refractive index detector and a column set of T6000 M and T3000 with THF as the mobile phase (1 mL/min flow rate). The polymers were dissolved in HPLC grade THF at 5.0 mg/mL and filtered through a PTFE syringe filter. The molecular weights and PDI were determined according to polystyrene standards. Differential scanning calorimetry (DSC) was conducted on a TA Instruments Q1000 Modulated Differential Scanning Calorimeter. Specifically, a heat/cool/heat cycle was conducted and T_g was measured on the final heating ramp. TGA was conducted with a TA Instruments Q500 Thermogravimetric Analyzer. Photorheology was

conducted at room temperature on a TA Instruments DHR3 Rheometer equipped with a UV curing accessory. Geometry was 20 mm parallel plate, composed of a disposable aluminum upper plate and an acrylic lower plate. A 365 nm UV filter was used, and the power output was 30 mW. Tensile testing and cyclic testing were conducted on Instron 5943 equipped with 50 N loading cell and Bluehill Universal software. Tensile testing was conducted at room temperature; dog bone samples were cured in a custom mold and washed with 1:1 EtOH/EtOAc for 2 days, followed by drying in vacuum for 24 h. Cyclic testing was conducted at 37 °C, with a strain range of 0%–20% and a strain rate of 125 mm/min; untreated dog-bone shaped samples were cut out using a custom build die and incubated at 37 °C for 1 h prior to cyclic testing. Yield strain was analyzed with ANOVA and followed by Tukey HSD posthoc test; the Young's modulus for 1 \times and 1.5 \times groups were analyzed with Student's t test, and ANOVA test was not used for the 2 \times group because the corresponding Young's modulus had a large standard deviation.

Degradation Study. A 20–30 mg amount of cured 1.95–2.00 mm thick PAPS slabs was placed in 1.5 mL Eppendorf tubes, and each combined weight (PAPS sample + Eppendorf tube) was measured on an analytical balance. One mL of 60 mM NaOH solution was then added, and the samples were incubated at room temperature for 4 h, 1 day, or 3 days, with gentle shaking on an orbital shaker. At the end of each time point, the samples were rinsed with water three times by pipetting up and down, and they were then lyophilized overnight. The mass remaining was calculated by subtracting the postdegradation dry weight from the predegradation dry weight.

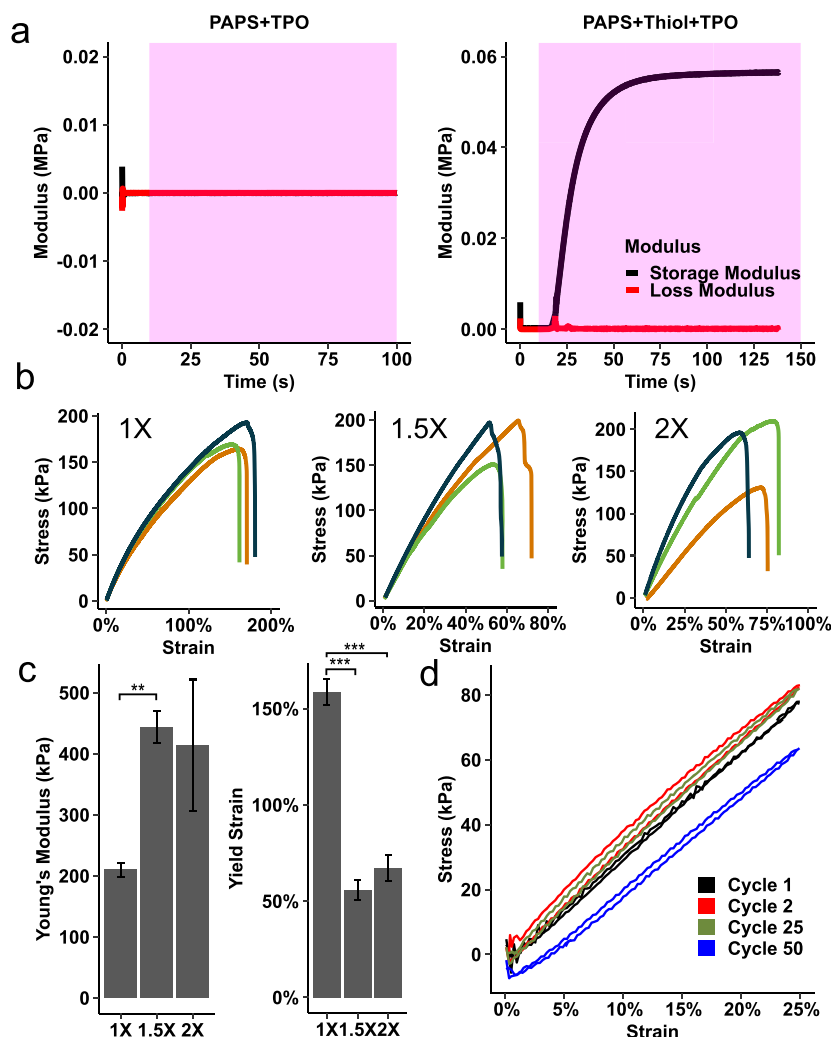


Figure 2. Mechanical properties of cured PAPS. (a) Photoreology of 20% PAPS ($M_n = 6458$ Da, PDI = 2.75) resin with or without thiol cross-linkers; the magenta-shaded box represents onset of UV exposure. (b) Uniaxial tensile testing of cured 20% PAPS. 0.5X, 1X, and 2X represent the molar excess of cross-linkers over alkynes ($n = 3$). (c) Young's modulus and yield strain across 20% PAPS samples cured with different concentrations of cross-linkers ($n = 3$). *** $p < 0.001$, ** $p < 0.01$. (d) Cyclic testing of 20% PAPS cured with 2X cross-linkers.

Cytotoxicity Study. According to ISO 10993-2012(E), PAPS strips were immersed in 70% ethanol for 24 h under agitation and then rinsed by sterile PBS six times before being soaked in an appropriate amount of endothelial cell growth medium. The PAPS extractions were obtained after soaking the PAPS strips in medium for 24 h with agitation. The medium with no PAPS served as control. The *in vitro* cytotoxicity assay was performed by adding extraction of PAPS to cultured human umbilical artery endothelial cells (HUAECs, 202-05N, Millipore Sigma) according to the manufacturer's instructions. HUAECs (passage 4) were subcultured using endothelial cell growth medium (EGM-2 BulletKit, CC-3156 & CC-4147, Lonza). The cells were harvested using trypsin/EDTA after reaching confluence and resuspended in medium to prepare a cell suspension of 5×10^3 cells per 150 μ L for cell seeding. The cells were allowed to attach for 3 h, then the medium was replaced by 150 μ L of PAPS extractions or control medium. The cells were incubated at 37 $^{\circ}$ C with 5% carbon dioxide. A Vybrant MTT Cell Proliferation Assay Kit (Invitrogen, Carlsbad, CA) was used to measure the cell metabolic activity of the HUAECs after an incubation of 1, 2, and 3 days. The absorbance was recorded using a SpectraMax

M3 microplate reader. At day 3, phase-contrast images were also taken on a Zeiss Axiovert 200 microscope equipped with a Dage 240 digital camera. All experiments were performed in quadruplicate.

RESULTS AND DISCUSSION

Synthesis. To generate a soft elastomer, we first reacted serinol with methyl 5-hexynoate neat to generate an alkyne-functionalized serinol derivative (Figure 1, Figure S1). Despite longer reaction time, melt polycondensation is simple to set up and avoids toxic catalysts and coupling agents (Figure 1a). A series of PAPS with 10% or 20% of alkyne groups were produced (Figure 1b). Polymer structure and quantitative integration of alkynes were confirmed by ^1H NMR (Figure 1b) and ^1H – ^1H COSY (Figure S3). A higher concentration of alkynes in PAPS not only resulted in higher molecular weights because AK has a higher molecular weight than 1,3-propanediol but also increased the PDI because AK monomers are more prone to side reactions (Figure 1b, entry 1 and entry 3). According to TGA, AK monomers started showing minimal weight loss at around 100 $^{\circ}$ C (Figure S2). We deduced that thermal degradation of AK generated free amines, which cross-

linked with other polymer chains via nucleophilic attacks. This also explained why extending the reaction time yielded polymers with significantly higher molecular weights and PDI (Figure 1b, entry 2).

Material Properties. Compared to MAA-based cross-linking, thiol–yne cross-linking is less sensitive to oxygen, which allows more flexibility in material manufacturing, especially in 3D printing where materials are constantly exposed to atmospheric oxygen.^{5,6} PAPS-dithiol solutions showed fast cross-linking kinetics, as evidenced by the exponential increase of storage modulus of the reaction mixture (PAPS+Thiol+TPO) within seconds of UV exposure in photorheology study (Figure 2). In the absence of thiol cross-linkers, UV-generated radical species did not cross-link the mixture (Figure 2a). Interestingly, prior to UV irradiation, the storage modulus of PAPS-dithiol solutions was higher than the loss modulus (Figure 2a), suggesting that premature thiol–yne addition transformed the mixture into a Bingham fluid, which behaves like a plastic until a threshold shear stress is reached. Premature thiol–yne addition is caused by peroxide impurities in the thiol cross-linkers, as well as by radicals spontaneously generated by atmospheric oxygen.⁹ Meanwhile, 10% PAPS ($M_n = 4274$ g/mol, PDI = 2.11) failed to cross-link into handleable samples in the same condition, potentially due to its lower molecular weight and lower percentage of alkyne groups.

We cross-linked 20% PAPS ($M_n = 6458$ Da, PDI = 2.75) with different equivalents of dithiols; the cross-linked network displayed two distinctive T_g values, both of which were slightly elevated at higher concentrations of dithiol cross-linkers (Table 1, Figure S4–S6). The absence of T_m suggested the

Table 1. Mechanical Properties of Crosslinked PAPS

thiol equiv	T_c (°C)	T_{g1} (°C)	T_{g2} (°C)	T_m (°C)	T_d (°C) ^b	E (kPa) ^c
0× ^a	−11.7	−41.5		19.6, 37.6	271	
1×		−41.5	4.83		301	210 ± 6
1.5×		−41.7	5.04		300	443 ± 13
2×		−44.2	5.71		301	413 ± 55

^aPure polymer without thiol addition. ^bDetermined by thermogravimetric analysis at 5% mass loss. ^cAutomatically determined by Instron Bluehill Universal software from uniaxial elongation tensile testing.

polymer was cross-linked into a thermoset, whose decreased chain mobility resulted in a higher T_{g2} . T_{g1} persisted across all four samples at roughly the same temperature. We attribute this to the sebacate-propanediol blocks in PAPS because they do not have any cross-linking point. Tensile testing and cyclic testing suggested that cured 20% PAPS was a soft elastomer and able to undergo cyclic loading with very small hysteresis (Figure 2b–d). Increasing the cross-linker concentration from 1× to 1.5× increased the Young's modulus of cross-linked 20% PAPS from 210 ± 6 kPa to 443 ± 13 kPa. However, a 2× cross-linker concentration did not further increase the Young's modulus (413 ± 55 kPa) (Figure 2b,c). Higher cross-linker concentrations (1.5× and 2×) also noticeably decreased the yield strain, suggesting that a lower cross-linking concentration (1×) made cured PAPS more elastic (Figure 2b,c). Furthermore, a diffusion NMR study of the reaction between 20% PAPS and dithiol in solution revealed that the diffusion coefficient of the resultant species inversely correlated to the cross-linker concentration (Figure 3).

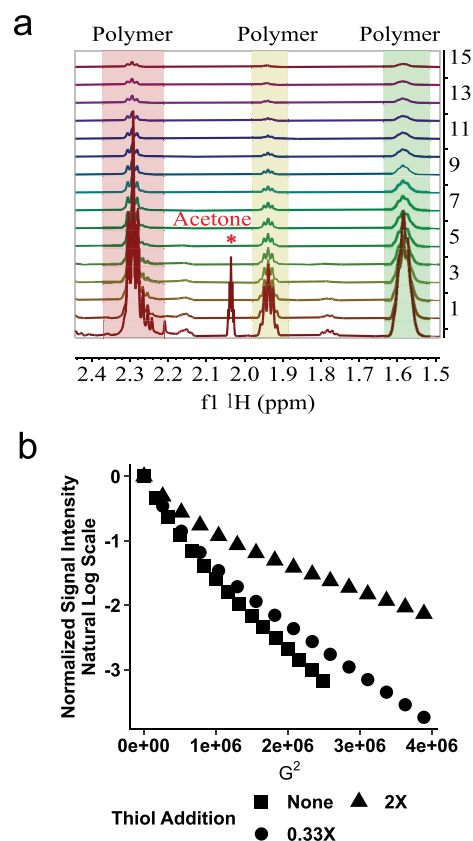


Figure 3. Diffusion NMR study of the cross-linking reaction. (a) Exponential decay of NMR signal intensity. It should be noted that the signal of small molecules (acetone) decayed to baseline level after the first iteration. (b) The signal decay was fitted with biexponential functions and linearized by taking the natural log; the diffusion coefficient is equal to the absolute value of the slope.

The degradation study showed that 1× PAPS degraded faster than 1.5× and 2× PAPS over a 3-day period (Figure 4). As for the chemical nature of the cross-linking, literature suggests that one thiol adds to one alkyne first to generate vinyl sulfide, which subsequently reacts with another thiol to generate an alkyl disulfide.⁶ Therefore, two polymer chains can be cross-linked by allyl sulfides, alkyl disulfides, or a combination of both (Figure 5a). NMR study of thiol–yne

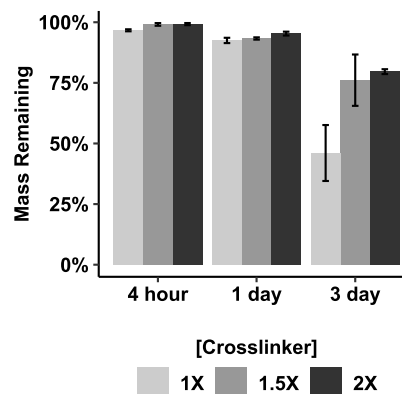


Figure 4. Degradation behavior of PAPS cross-linked with different cross-linker concentrations. Two way ANOVA analysis showed statistically significant effects of cross-linker concentration ($p < 0.05$) and degradation time ($p < 0.001$) on the degradation kinetic.

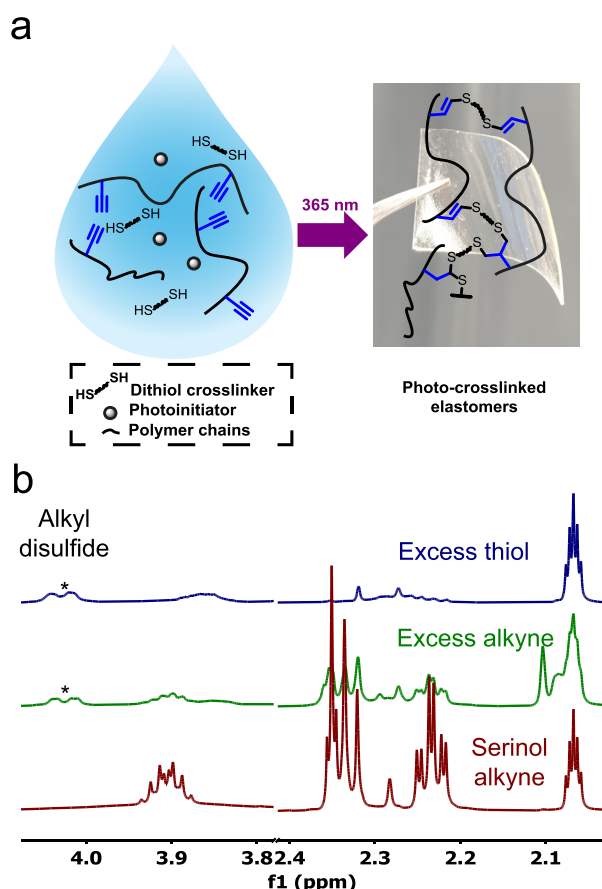


Figure 5. Mechanism of thiol–yne photo-cross-linking of PAPS. (a) Alkynes react with either 1 or 2 equiv of thiols to form vinyl sulfides or alkyl disulfides. (b) NMR study of serinol alkyne monomers reacting with different amounts of 2,2'-(ethylenedioxy)diethanethiol. Signal intensity decreased overall as polymeric species formed, but alkyl disulfides appeared as a broad doublet at 4.01 ppm.

reaction between serinol alkyne monomer and 2,2'-(ethylenedioxy)diethanethiol revealed the formation of alkyl disulfides (broad doublet, 4.01 ppm); vinyl sulfides did not form in a significant amount because we did not observe new peaks forming at 4–6 ppm (Figure 5b). Therefore, alkyl disulfides make up a majority of the cross-links, which agrees with a previous observation in the literature, where thiols more preferentially added to vinyl sulfides than to alkynes.⁶ We also attempted to investigate the chemical nature of cross-linking by FT-IR of cross-linked PAPS. However, IR has low sensitivity to compositional changes so we could not discern any significant change in bonding due to the low concentration of alkynes in the polymers (Figure S7).

Lastly, we examined the cytocompatibility of extracts of cross-linked PAPS using MTT assay. HUAECs were cultured in endothelial cell culture media containing extract of cross-linked 20% PAPS. We chose PAPS with the highest percentage of alkyne to evaluate if alkyne-functionalized serinol derivatives are toxic to human cells. HUAECs cultured in the polymer extract showed similar metabolic activity compared to those cultured in fresh cell media (Figure 6a). According to the micrograph, HUAECs in the treated group did not undergo morphological change (Figure 6b). Overall, the data suggested good cytocompatibility of PAPS.

Perspectives and Potential Applications. The fast cross-linking kinetic opens the possibility of using PAPS

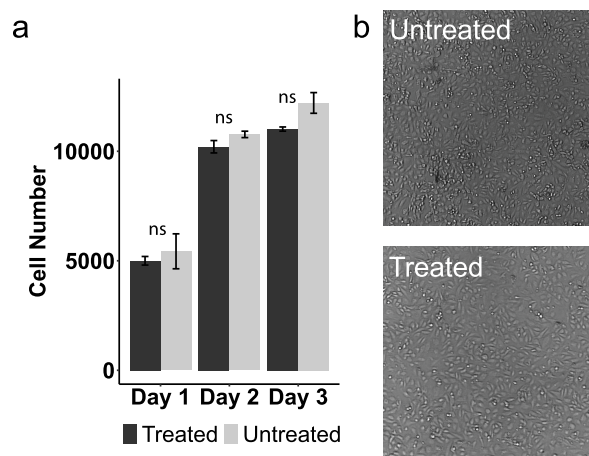


Figure 6. Cytocompatibility study of cross-linked PAPS using HUAECs. (a) MTT assay of HUAECs treated with PAPS extract (treated group) or fresh endothelial cell media (untreated group), $n = 4$. The difference between treated and untreated in each time point was analyzed by Student's t test; ns: not significant. (b) Cell morphology at day 3.

solution as a photopolymerizable resin for DLP and other fabrication methods such as electrospinning. For DLP, alkyne-bearing photopolymerizable resins have shown good resolution and oxygen tolerance.^{6,7,10,11} Because of the step-growth mechanism, thiol–yne resins also demonstrate reduced shrinkage stress during cross-linking, which is crucial to the integrity of printed objects.¹² Most of these precedents use multifunctional small molecule alkyne monomers, which necessitate a high amount of thiol cross-linkers that are potentially cytotoxic and often foul smelling.^{10,12,13} In addition, the printed objects are stiff due to high cross-linking density, which precludes them from soft material applications.^{12,13} In contrast, photo-crosslinked PAPS is a soft elastomer because PAPS can be crosslinked by a significantly lower amount of thiol crosslinkers. As for electrospinning, the polymer must reach a threshold molecular weight to generate sufficient chain entanglement for fiber formation.¹⁴ Fiber morphology also depends on molecular weights: electrospun fibers of poly(vinyl alcohol) at 9000–13 000 g/mol showed a bead-on-string structure, suggesting solvent jet instability, while increasing the molecular weight to 31 000–50 000 g/mol yielded fibers without bead formation.¹⁵ High-molecular-weight additives, by acting as carriers, also promote the electrospinning of polymers with low molecular weight or low T_m , which are challenging to electrospin by themselves.¹⁶ For instance, PGS was coelectrospun with high molecular weight poly(vinyl alcohol), which was removed by water after PGS was cured into a thermoset, resulting in a thermoset PGS fiber.^{16,17} For PAPS, we deem an *in situ* cross-linking during the fiber formation offers sufficient chain entanglement. Previously, low molecular weight poly(propylene fumarate) with M_n ranging from merely 400 g/mol to 2000 g/mol successfully generated microfiber in this fashion.¹⁸

Nevertheless, thiol–yne photocurable resins have their limitations. First, the resins can present significant synthetic challenges. MAA are commercially available as both anhydrides and acyl chlorides for easy modifications of materials with complex structures under mild conditions.^{2,19,20} In contrast, alkynylation often requires organolithiums or Grignard reagents, transition metal-catalyzed cross-coupling reagents,

and extremely hazardous reagents such as propargyl halide or propargyl alcohol that can perform nucleophilic substitution or esterification;^{21–23} these synthetic techniques are not amenable to generating biomedical materials where toxicity is a major concern. Although we used a transesterification-like reaction with a relatively benign alkyne substrate, its high cost might hinder downstream development and commercialization. Second, while thiol–yne resins have a rapid cross-linking kinetic, they are also prone to spontaneous crosslinking reactions, which are triggered by the formation of radical species and the base-catalyzed nucleophilic addition of thiols to alkynes.⁹ Small molecule stabilizers inhibit the side reactions to some degree, but they might reduce the cytocompatibility.⁹ Compared to primary thiol cross-linkers, secondary thiol cross-linkers have a significantly improved shelf life due to the additional steric hindrance.¹³ In our design, we lowered the concentration of thiols and alkynes by functionalizing the polymer with alkyne groups. We expect the reduced concentration of reactive groups, as well as the increased viscosity of resin mixture compared to small molecule resins, can limit the extent of side reactions. Third, melt polycondensation of PAPS is time-consuming and incompatible with heat labile compounds, nor is it amenable to functional groups prone to thermo-cross-linking. For instance, we replaced a fraction of 1,3-propanediol with glycerol to make a material that has elastomeric properties similar to those of PGS. However, the resulting polymers inevitably cross-linked during synthesis due to the presence of secondary OH groups (data not shown).

As research progresses with thiol–yne chemistry, we expect limitations will eventually be less a challenge. The rapid kinetic is both an advantage and a point for caution in handling and storage. Modern catalysts overcome the third limitation by providing a mild reaction condition. Slavko and Taylor employed boron catalysts to produce PGS with less than 1% branching on the secondary OH, which in return yielded a lower PDI and a higher M_n compared to traditionally made PGS.²⁴ However, their method requires diacyl chlorides as the monomers, which have limited commercial availability for various dicarboxylic acids. Diacyl chlorides also have limited shelf life due to their sensitivity to moisture. In contrast, the Coates group developed metal–salen catalysts that generate narrowly dispersed, high molecular weight polyesters from commercially available cyclic acid anhydrides and epoxides.^{25–27} However, all our attempts to generate cyclic, monomeric sebacic anhydride yielded poly(sebacic anhydride), which agrees with published results.^{28,29} Moreover, the binary metal–salen catalysts have a narrow substrate scope: protic functional groups greatly retard the catalyst activity.^{26,27} The Coates group later developed a bifunctional metal–salen catalyst whose activity is not impacted by protic functional groups.^{25,30} The protic functional groups act as chain transfer agents (CTAs) to initiate new chains.³⁰ By using various CTAs, this bifunctional catalyst can lead to polymers with complex architectures such as star polymers and ABA block copolymers.³⁰ Although monomers with protic functional groups can still lead to undesired branching or even cross-linking, we will investigate means to synthesize a diverse class of low toxicity polyesters with high M_n and narrow PDI from anhydrides and epoxides with photo-cross-linkable functional groups.

CONCLUSION

PAPS, an alkyne-functionalized biodegradable polyester, is easily synthesized via melt polycondensation. PAPS resin shows facile cross-linking kinetic under UV, and we intend to exploit it in applications such as electrospinning and DLP. Cross-linked PAPS is a degradable, soft elastomer, and its mechanical properties approximate those of human soft tissues. The material is cytocompatible with endothelial cells. For future work, we will focus on increasing the molecular weight of PAPS to decrease the concentration of alkynes needed to photo-cross-link PAPS. Furthermore, we will formulate PAPS with a proper solvent to yield a low toxicity DLP resin amenable to manufacturing at room temperature, as well as evaluating *in vivo* compatibility of the printed objects. We will look beyond PAPS and utilize other synthetic methods to generate polyesters with different architectures to broaden the scope of applications.

ASSOCIATED CONTENT

Supporting Information

The Supporting Information is available free of charge at <https://pubs.acs.org/doi/10.1021/acsomega.2c00272>.

Figure S1: NMR of alkyne-functionalized serinol monomer; Figure S2: TGA of alkyne-functionalized serinol monomer; Figure S3: ¹H-¹H COSY of 20% PAPS in acetone-d₆; Figures S4–6: DSC of 20% PAPS crosslinked with thiol crosslinkers at various equivalents; Figure S7: IR of alkyne serinol monomers, 20% PAPS, and crosslinked PAPS (PDF)

AUTHOR INFORMATION

Corresponding Authors

Xiaochu Ding – Department of Chemistry, Michigan Technological University, Houghton, Michigan 49931, United States; Email: xding@mtu.edu

Yadong Wang – Meinig School of Biomedical Engineering, College of Engineering, Cornell University, Ithaca, New York 14853, United States; orcid.org/0000-0003-2067-382X; Email: yw839@cornell.edu

Authors

Warrick Ma – Department of Chemistry and Chemical Biology, College of Arts and Sciences, Cornell University, Ithaca, New York 14853, United States

Ying Chen – Meinig School of Biomedical Engineering, College of Engineering, Cornell University, Ithaca, New York 14853, United States; orcid.org/0000-0002-0333-2217

Complete contact information is available at: <https://pubs.acs.org/doi/10.1021/acsomega.2c00272>

Notes

The authors declare no competing financial interest.

ACKNOWLEDGMENTS

The authors thank Paula G. Miller for assistance in the cytocompatibility study, Dr. David B. Collum for discussion on monomer synthesis, and Dr. Anthony M. Condo for assistance in data acquisition. W.M. also remembers Thomas R. Rutledge (b.1964–d.2020) for his mentorship and engaging conversations. This work made use of the CCMR Shared Experimental Facilities and the NMR Facility at Cornell University, which are supported by the NSF (DMR-1719875).

and CHE-1531632, respectively). This work was supported by a startup fund from Cornell University.

REFERENCES

- (1) Nijst, C. L. E.; Bruggeman, J. P.; Karp, J. M.; Ferreira, L.; Zumbuehl, A.; Bettinger, C. J.; Langer, R. Synthesis and Characterization of Photocurable Elastomers from Poly(glycerol-co-sebacate). *Biomacromolecules* **2007**, *8*, 3067–3073.
- (2) Yeh, Y.-C.; Highley, C. B.; Ouyang, L.; Burdick, J. A. 3D printing of photocurable poly(glycerol sebacate) elastomers. *Biofabrication* **2016**, *8*, 045004.
- (3) Yeh, Y.-C.; Ouyang, L.; Highley, C. B.; Burdick, J. A. Norbornene-modified poly(glycerol sebacate) as a photocurable and biodegradable elastomer. *Polym. Chem.* **2017**, *8*, 5091.
- (4) Juránová, J. Illuminating the cellular and molecular mechanism of the potential toxicity of methacrylate monomers used in biomaterials. *Drug and Chemical Toxicology* **2020**, *43*, 266–278.
- (5) Bagheri, A.; Jin, J. Photopolymerization in 3D Printing. *ACS Appl. Polym. Mater.* **2019**, *1*, 593–611.
- (6) Fairbanks, B. D.; Scott, T. F.; Kloxin, C. J.; Anseth, K. S.; Bowman, C. N. Thiol-Yne Photopolymerizations: Novel Mechanism, Kinetics, and Step-Growth Formation of Highly Cross-Linked Networks. *Macromolecules* **2009**, *42*, 211–217.
- (7) Roppolo, I.; Frascella, F.; Gastaldi, M.; Castellino, M.; Ciubini, B.; Barolo, C.; Scaltrito, L.; Nicosia, C.; Zanetti, M.; Chiappone, A. Thiol-yne chemistry for 3D printing: exploiting an off-stoichiometric route for selective functionalization of 3D objects. *Polym. Chem.* **2019**, *10*, 5950–5958.
- (8) Chen, Y.; Miller, P. G.; Ding, X.; Stowell, C. E. T.; Kelly, K. M.; Wang, Y. Chelation Crosslinking of Biodegradable Elastomers. *Adv. Mater.* **2020**, *32*, 2003761.
- (9) Oesterreicher, A.; Moser, A.; Edler, M.; Griesser, H.; Schlögl, S.; Pichelmayer, M.; Griesser, T. Investigating Photocurable Thiol-Yne Resins for Biomedical Materials. *Macromol. Mater. Eng.* **2017**, *302*, 1600450.
- (10) Oesterreicher, A.; Wiener, J.; Roth, M.; Moser, A.; Gmeiner, R.; Edler, M.; Pinter, G.; Griesser, T. Tough and degradable photopolymers derived from alkyne monomers for 3D printing of biomedical materials. *Polym. Chem.* **2016**, *7*, 5169–5180.
- (11) Lu, H.; Carioscia, J. A.; Stansbury, J. W.; Bowman, C. N. Investigations of step-growth thiol-ene polymerizations for novel dental restoratives. *Dental Materials* **2005**, *21*, 1129–1136.
- (12) Ye, S.; Cramer, N. B.; Smith, I. R.; Voigt, K. R.; Bowman, C. N. Reaction Kinetics and Reduced Shrinkage Stress of Thiol-Yne-Methacrylate and Thiol-Yne-Acrylate Ternary Systems. *Macromolecules* **2011**, *44*, 9084–9090.
- (13) Chen, L.; Wu, Q.; Wei, G.; Liu, R.; Li, Z. Highly stable thiol-ene systems: from their structure-property relationship to DLP 3D printing. *J. Mater. Chem. C* **2018**, *6*, 11561–11568.
- (14) Shenoy, S. L.; Bates, W. D.; Frisch, H. L.; Wnek, G. E. Role of chain entanglements on fiber formation during electrospinning of polymer solutions: good solvent, non-specific polymer-polymer interaction limit. *Polymer* **2005**, *46*, 3372–3384.
- (15) Koski, A.; Yim, K.; Shivkumar, S. Effect of molecular weight on fibrous PVA produced by electrospinning. *Mater. Lett.* **2004**, *58*, 493–497.
- (16) Jeffries, E. M.; Allen, R. A.; Gao, J.; Pesce, M.; Wang, Y. Highly elastic and suturable electrospun poly(glycerol sebacate) fibrous scaffolds. *Acta biomaterialia* **2015**, *18*, 30–39.
- (17) Stowell, C. E. T.; Wang, Y. Quickening: Translational design of resorbable synthetic vascular grafts. *Biomaterials* **2018**, *173*, 71–86.
- (18) Cicotte, K. N.; Hedberg-Dirk, E. L.; Dirk, S. M. Synthesis and electrospun fiber mats of low Tg poly(propylene fumarate-co-propylene maleate). *J. Appl. Polym. Sci.* **2010**, *117*, 1984–1991.
- (19) Xiao, S.; Zhao, T.; Wang, J.; Wang, C.; Du, J.; Ying, L.; Lin, J.; Zhang, C.; Hu, W.; Wang, L.; Xu, K. Gelatin Methacrylate (GelMA)-Based Hydrogels for Cell Transplantation: an Effective Strategy for Tissue Engineering. *Stem Cell Rev. Rep.* **2019**, *15*, 664–679.
- (20) Schuurmans, C.; Mihajlovic, M.; Hiemstra, C.; Ito, K.; Hennink, W. E.; Vermonden, T. Hyaluronic acid and chondroitin sulfate (meth)acrylate-based hydrogels for tissue engineering: Synthesis, characteristics and pre-clinical evaluation. *Biomaterials* **2021**, *268*, 120602.
- (21) He, H.; Zhang, Y.; Gao, C.; Wu, J. ‘Clicked’ magnetic nanohybrids with a soft polymer interlayer. *Chem. Commun.* **2009**, 1655–1657.
- (22) Le Vaillant, F.; Waser, J. Alkynylation of radicals: spotlight on the “Third Way” to transfer triple bonds. *Chem. Sci.* **2019**, *10*, 8909–8923.
- (23) Baralle, A.; Yorimitsu, H.; Osuka, A. Pd-NHC-Catalyzed Alkynylation of General Aryl Sulfides with Alkynyl Grignard Reagents. *Chem. Eur. J.* **2016**, *22*, 10768–10772.
- (24) Slavko, E.; Taylor, M. S. Catalyst-controlled polycondensation of glycerol with diacyl chlorides: linear polyesters from a trifunctional monomer. *Chem. Sci.* **2017**, *8*, 7106–7111.
- (25) Abel, B. A.; Lidston, C. A. L.; Coates, G. W. Mechanism-Inspired Design of Bifunctional Catalysts for the Alternating Ring-Opening Copolymerization of Epoxides and Cyclic Anhydrides. *J. Am. Chem. Soc.* **2019**, *141*, 12760–12769.
- (26) Sanford, M. J.; Zee, N. J. V.; Coates, G. W. Reversible-deactivation anionic alternating ring-opening copolymerization of epoxides and cyclic anhydrides: access to orthogonally functionalizable multiblock aliphatic polyesters. *Chem. Sci.* **2018**, *9*, 134–142.
- (27) Fieser, M. E.; Sanford, M. J.; Mitchell, L. A.; Dunbar, C. R.; Mandal, M.; Van Zee, N. J.; Urness, D. M.; Cramer, C. J.; Coates, G. W.; Tolman, W. B. Mechanistic Insights into the Alternating Copolymerization of Epoxides and Cyclic Anhydrides Using a (Salph)AlCl and Iminium Salt Catalytic System. *J. Am. Chem. Soc.* **2017**, *139*, 15222–15231.
- (28) Hill, J. W.; Carothers, W. H. STUDIES OF POLYMERIZATION AND RING FORMATION. XIV. A LINEAR SUPER-POLYANHYDRIDE AND A CYCLIC DIMERIC ANHYDRIDE FROM SEBACIC ACID. *J. Am. Chem. Soc.* **1932**, *54*, 1569–1579.
- (29) Hill, J. W.; Carothers, W. H. Studies of Polymerization and Ring Formation. XIX.1 Many-Membered Cyclic Anhydrides. *J. Am. Chem. Soc.* **1933**, *55*, 5023–5031.
- (30) Lidston, C. A. L.; Abel, B. A.; Coates, G. W. Bifunctional Catalysis Prevents Inhibition in Reversible-Deactivation Ring-Opening Copolymerizations of Epoxides and Cyclic Anhydrides. *J. Am. Chem. Soc.* **2020**, *142*, 20161–20169.